Electron-correlation-induced interchange of lifetime broadenings of $5s^{-1}$ multiplet states in atomic Cs

L. Partanen,[1,*] J. Schulz,[2] M. Holappa,[1] H. Aksela,[1] and S. Aksela[1]

[1]*Department of Physical Sciences, University of Oulu, P.O. Box 3000, 90014 Oulu, Finland*
[2]*Centre for Free-Electron Laser Science at DESY, 22603 Hamburg, Germany*

The lifetime broadenings of the most intense $5s$ photolines of Cs were studied. The aim of this study was to understand the origin of the remarkable differences in the lifetime widths of different $5s^{-1}$ multiplet states. The $5s$ photoelectron spectra of the $6s \rightarrow 6p_{1/2,3/2}$ laser-excited states are presented in the binding energy region of 30–34 eV showing the main $5s$ photolines of the ground state and laser-excited states as well as the $5s5p^66p$ shakeup satellites. The lifetime widths of the states were determined. The Hartree-Fock calculations were carried out to predict the $5s$ photoelectron spectrum. The lifetime broadenings of the $5s$ photolines were found to be due to the transition rates of the subsequent Coster-Kronig transitions to the $5s^25p^5$ states. It was found that a straightforward single-configuration explanation cannot be given for the lifetime differences. Instead, electron correlation plays an essential role and the lifetime broadenings were found to be predicted well only when configuration interaction between the $5s^{-1}$ and $5p^{-2}5d$ configurations is taking into account.

I. INTRODUCTION

In open shell atoms, the coupling between the core hole created in photoionization and the open valence shell produces a multiplet structure in the photoelectron spectra. All atomic states (multiplets) can decay by emitting an Auger electron. The decay rates are state dependent. For example, the Auger lifetime widths of the $4d^{-1}$ photoionized states were found to vary strongly between the multiplets in heavy rare-earth elements (see, e.g., [1] and references therein). The multiplet-dependent super-Coster-Kronig decay rates were found to be responsible for large variations in level widths [1–4].

Recently, Schulz *et al.* [5] reported clearly different lifetime broadenings for the $4s$ ionized states of Rb. The lifetime broadenings of the $4s4p^65s$ ^1S and ^3S multiplets were found to differ, with the singlet state being considerably broader than the triplet state. The finding was argued to be due to the fact that the Coster-Kronig (CK) transition rates to the Rb^{2+} $4s^24p^5$ ^2P states are high from the singlet state when the spins of $4s$ and $5s$ electrons are oriented antiparallel to each other. Instead, the spin-flip process during the Auger decay is less probable leading to low Auger transition rate from the triplet state. Thus, the Auger decay rates result in broad $4s4p^65s$ ^1S and narrow $4s4p^65s$ ^3S photolines. Also the $4s$ photolines of the $5s$ to $5p_{1/2,3/2}$ laser-excited Rb atoms were studied in [5]. The $4s4p^65p$ ^1P photoline was found to be considerably broader than the $4s4p^65p$ ^3P lines. This was assumed to be due to the fact that the widths of the $4s4p^65p$ states depend strongly on the spin-spin coupling between the $4s$ and $5p$ electrons. However, a straightforward explanation for the difference in linewidths could not be given in [5], but a need for further theoretical studies including the possible configuration interaction (CI) with the $4s^24p^44d5p$ states was pointed out.

In this study, natural widths of the $5s$ photolines of Cs were investigated in detail and compared to the $4s$ photolines of Rb. The valence electron configuration of the Cs atom $5s^25p^66s$ is similar to the Rb atom, so similar behavior of lifetime broadenings was expected. The $5s$ photoelectron spectrum of Cs was measured for the ground state and for the $6s$ to $6p_{1/2,3/2}$ excited states. The lifetime widths of the Cs photolines were determined. The decay probabilities of CK transitions following the photoionization in Rb and Cs were calculated with the Hartree-Fock (HF) approximation. The effect of electron correlation on natural widths of $5s^{-1}$ states was studied by comparing the Auger amplitudes in the single-configuration (SC) and CI approximations. The experimental lifetime widths were compared with theoretical estimates. As will be shown below, our detailed analysis allowed us to arrive at a better understanding of the effects, which play a prominent role in determining the lifetime widths of the singlet and triplet states of alkali atoms Cs and Rb.

II. EXPERIMENTS

The photoelectron spectra from free Cs atoms were measured at the I411 beamline in the MAX II synchrotron radiation storage ring with the photon energy of 72 eV. A beam of free Cs atoms was produced in a resistively heated oven. A temperature of 125 °C was sufficient to produce a vapor pressure of 10^{-3} mbar in the crucible. The beamline exit slit was set to 50 μm. A SES-100 electron energy analyzer with 0.4 mm curved entrance slit and fixed pass energy of 20 eV was used providing the analyzer width (full width at half maximum) of 43 meV. The analyzer line profile was determined with the aid of the Xe $5p$ photolines. The Gaussian contribution of the analyzer width was 37 meV and the Lorentzian contribution was about 11 meV. Cesium atoms were excited with a continuous-wave Ti:sapphire laser at wavelengths of 894.3 and 852.1 nm corresponding to the $6s \rightarrow 6p_{1/2}$ and $6s \rightarrow 6p_{3/2}$ resonances, respectively. The bind-

*leena.partanen@oulu.fi
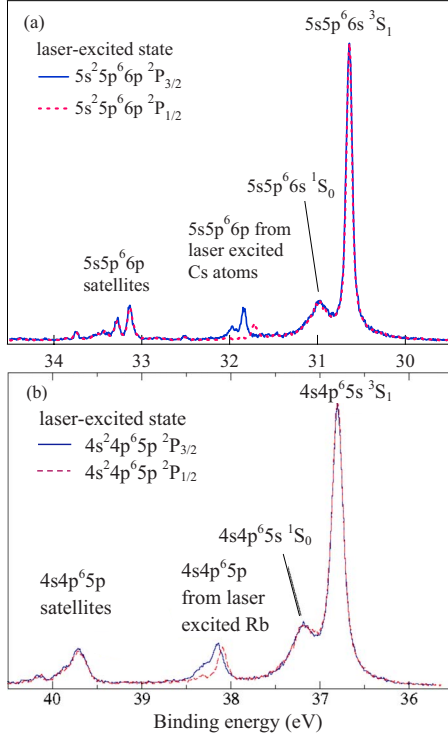
FIG. 1. (Color online) (a) 5s photoelectron spectrum from laser-excited Cs. (b) 4s photoelectron spectrum from laser-excited Rb. In the blue solid spectrum the laser is tuned to the $ns \rightarrow np_{3/2}$ excitation and the red dashed spectrum depicts the $ns \rightarrow np_{1/2}$ excitation ($n=6$ for Cs and $n=5$ for Rb).

ing energy calibration was done by measuring the $3p$ photolines of argon together with the Cs spectrum.

The experimental $5s$ photoelectron spectra of the $6s$ to $6p$ laser-excited Cs atoms in the binding energy region of 30.0–34.0 eV are depicted in Fig. 1(a). The $5s5p^66p$ photolines originating from the $5s^25p^66p\ ^2P_{1/2}$ and $^2P_{3/2}$ laser-excited states are shown at the binding energy region of 31.7–32.0 eV. Because laser light excites only a part of sample gas atoms (approximately 5–10 %), the most intense peaks in both spectra are the $5s5p^66s\ ^1S_0$ and $^3S_1$ photoelectron lines at the binding energies of 30.98 and 30.64 eV, respectively. The lines lying at the binding energy region of 33.0–34.0 eV are shakeup satellites originating from the $5s^25p^66s\ ^2S$ to $5s5p^66p$ transitions. Figure 1(b) shows the corresponding $4s$ photoelectron spectrum of Rb in the binding energy region of 35.5–40.5 eV taken from [5]. The Cs and Rb spectra resemble each other. For the $nsnp^6ms$ states ($n=4$, $m=5$ for Rb and $n=5$, $m=6$ for Cs), the $^3S_1$ state has about twice as much intensity as the $^1S_0$ state. The binding energy splitting between the singlet and triplet multiplets is 0.34 eV for Cs and 0.38 eV for Rb.

The experimental lifetime widths of the Cs spectra were determined by fitting the spectra with peaks having Voigt profiles. The fitting results without the linear background line are shown in Fig. 2(b) and the lifetime broadenings are given in Table I. The broadenings originating from photon band and the analyzer were subtracted from the tabulated values. For comparison, the lifetime broadenings of the Rb $4s$ photolines taken from [5] are also given in Table I.
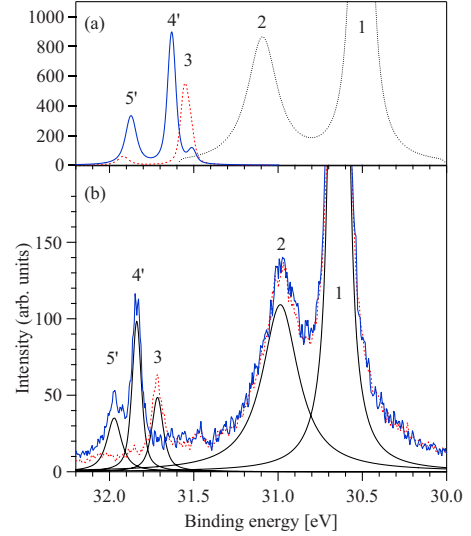
FIG. 2. (Color online) (a) Calculated and (b) experimental $5s$ photoelectron spectrum of laser-excited Cs. The upper panel shows $5s5p^66s$ (black dotted curve), $5s5p^66p_{1/2}$ (red dashed curve), and $5s5p^66p_{3/2}$ (blue solid curve) lines. The lower panel shows fitted experimental lines (black solid curve), $6s \rightarrow 6p_{1/2}$ laser-excited lines (red dashed curve), and $6s \rightarrow 6p_{3/2}$ laser-excited lines (blue solid curve).

III. CALCULATIONS

The binding energies, intensities, and widths of the $5s$ photolines of the ground state and $6s \rightarrow 6p$ laser-excited Cs atom were calculated with the COWAN code [6]. The HF wave functions with relativistic corrections (HFR) were computed in the intermediate coupling scheme for the states involved in the studies transitions. The HF Coulomb radial integral values for the states having a $6s$ electron were scaled down by 10% for better correspondence between the calculated and the experimental energies while the radial integrals for the $6s$ to $6p$ laser-excited states were not scaled. The ground state of a Cs atom was described with the SC $[Kr]4d^{10}5s^25p^66s$. The CI method was applied when predicting the wave functions for the $5s^{-1}$ states by mixing the

TABLE I. Experimental and calculated lifetime widths of the $nsnp^6ms\ ^3S_1,\ ^1S_0$ and laser-excited $nsnp^6mp\ ^3P_{0,1,2},\ ^1P_1$ states of Rb ($n=4, m=5$) and Cs ($n=5, m=6$). Error limits for the experimental values are given for Cs.

		Cesium		Rubidium	
Label	State	Expt. (meV)	Calc. (meV)	Expt.[a] (meV)	Calc. (meV)
1	$^3S_1$	55 ± 10	62	118	103
2	$^1S_0$	250 ± 30	206	330	303
3	$^3P_0$	40 ± 10	34	84	65
3	$^3P_1$		38		67
4	$^3P_2$	35 ± 10	45	71	71
5	$^1P_1$	80 ± 10	73	280	87

[a]Reference [5].

TABLE II. Experimental and calculated binding energies of the $5s5p^66s$ and the laser-excited $5s5p^66p$ states. Relative intensities for the $5s5p^66p$ states are also given. Error limits for the experimental values are given in parentheses in the third row.

Label Error limit	State	Binding energy (eV)		Rel. intensity	
		Expt. (± 0.01)	Calc.	Expt. (± 5)	Calc.
Laser off					
1	$5s5p^66s\ ^3S_1$	30.64	30.50	70	74
2	$5s5p^66s\ ^1S_0$	30.98	31.09	30	26
Laser on, $6s \rightarrow 6p_{1/2}$					
3 $\Big\{$	$5s5p^66p\ ^3P_0$	31.72	31.52	29	8
	$5s5p^66p\ ^3P_1$		31.56		21
4	$5s5p^66p\ ^3P_2$		31.68		0
5	$5s5p^66p\ ^1P_1$		31.92		4
Laser on, $6s \rightarrow 6p_{3/2}$					
3' $\Big\{$	$5s5p^66p\ ^3P_0$		31.47		
	$5s5p^66p\ ^3P_1$		31.51		
4'	$5s5p^66p\ ^3P_2$	31.84	31.63	46	42
5'	$5s5p^66p\ ^1P_1$	31.97	31.87	25	22

[Kr]$4d^{10}5s5p^66l$ and [Kr]$4d^{10}5s^25p^45d6l$ ($l=s$ or p) states for nonexcited and laser-excited atoms, respectively.

The binding energies of the $5s$ ionized states with respect to the ground state and to the $6s \rightarrow 6p_{1/2,3/2}$ excited states determined from the CI calculations are given in Table II. The dipole transition probabilities from the [Kr]$4d^{10}5s^25p^66s\ ^2S_{1/2}$ state to the [Kr]$4d^{10}5s5p^66s\ ^1S_0$, $^3S_1$ states and from the [Kr]$4d^{10}5s^25p^66p\ ^2P_{1/2,3/2}$ initial states to the [Kr]$4d^{10}5s5p^66p\ ^1P_1$, $^3P_{0,1,2}$ final states were also calculated, and the relative intensities (i.e., the distribution of transition rate between the $5s^{-1}$ states) are also given in Table II. In order to identify the photolines originating from the laser-excited initial states, the calculated spectrum was simulated and compared with the experimental one in Fig. 2. The assignments for peaks 1–5 are given in Table II. The labels with prime indicate the $5s5p^66p_{3/2}$ photolines while the labels without prime indicate the $5s5p^66s$ and $5s5p^66p_{1/2}$ photolines. The energy splitting between the $5s5p^66p\ ^3P_0$ and $^3P_1$ states is below the experimental resolution, so they are treated here as a single peak labeled as 3 while the $^3P_2$ (peak 4) and $^1P_1$ (peak 5) states appear separate from other peaks.

The lifetime broadenings were computed for peaks 1–5. The lifetimes of the $5s$ ionized states were assumed to be mainly determined by the CK transitions to the [Kr]$4d^{10}5s^25p^5\ ^2P_{1/2,3/2}$ states. The Auger transition calculations were carried out both in SC approximation and by taking CI between $5s^{-1}$ and $5p^{-2}5d$ into account. For comparison, similar calculations were carried out also for Rb atom. In Auger calculations, the HFR continuum orbitals were generated in the configuration-average potentials of each final electron configuration. The energies of continuum electrons

were taken as a difference between the configuration-average energies of initial and final electron configurations. The results are given and discussed in Sec. IV.

Within the two-step model and using the CI formalism, the Auger transition rate between the intermediate level β (initial state of Auger decay) and the final level f is proportional to a sum of the squared Auger amplitudes between intermediate- and final-state components,

$$T_{f\beta}(J_f, J_\beta) = 2\pi \sum_{l_A j_A} \left| \sum_\mu \sum_\nu c_{f\mu} c_{\beta\nu} M_{f\beta}^{\mu\nu} \right|^2, \qquad (1)$$

where $M_{f\beta}^{\mu\nu} = \langle \Phi_\mu(J_f)\varepsilon_A l_A j_A; J_\beta \| V \| \Phi_\nu(J_\beta) \rangle$ is a Coulomb matrix element and where a continuum electron $\varepsilon_A l_A j_A$ is coupled to the final ionic state to form the final state of Auger transition with one electron in the continuum [7]. The coefficients $c_{f\mu}$ and $c_{\beta\nu}$ are the CI mixing coefficients for each basis state μ having J_f in the final state f and ν having J_β in the photoionized intermediate state β, respectively. Since there are only two nonmixing $5s^25p^5$, $^2P_{1/2,3/2}$ final states $c_{f\mu}$ is 1.

IV. DISCUSSION

For Cs and Rb, the singlet lines are much broader than the triplet lines both in the peak structures 1 and 2 and 3–5 (see Table I). The photolines of Rb atom are about two times broader than the corresponding Cs lines indicating more rapid de-excitation processes for Rb. In order to understand the origin of the observed different lifetime widths of singlet and triplet states, the Auger transition rates from the $5s5p^66s$ and $5s5p^66p$ initial states to the $5s^25p^5\ ^2P_{1/2,3/2}$ final states of Cs were analyzed in details.

First, the Auger transition rates computed with the SC approximation were examined. According to Eq. (1), the Auger transition rates depend on the $\langle 5s\varepsilon p; J_f \| V \| 5p6s; J_f \rangle$, $\langle 5p\varepsilon s; J_f \| V \| 5d6p; J_f \rangle$, and $\langle 5p\varepsilon d; J_f \| V \| 5d6p; J_f \rangle$ Coulomb matrix elements, which are given in Table III in column $M_{f\beta}^{\mu\nu}$. In the intermediate coupling scheme, the states having the same parity and angular momenta J are allowed to mix, e.g., the $5s5p^66p\ ^3P_1$ and $^1P_1$ states that couple together. The Auger amplitude $c_{f\mu} c_{\beta\nu} M_{f\beta}^{\mu\nu}$ is the Auger matrix element multiplied by the intermediate coupling eigenvector coefficient of initial state (not given in Table III) while $c_{f\mu} = 1$. The transition rate is then directly proportional to the square of the sum over all contributing Auger amplitudes, which is the value given in the row labeled with $|\sum_\mu \sum_\nu c_{f\mu} c_{\beta\nu} M_{f\beta}^{\mu\nu}|^2$ SC.

According to the SC calculations the Auger transition probability of the $5s^15p^66s\ ^3S_1$ triplet state (peak 1) is over 40 times higher than the Auger transition probability of the singlet state $5s^15p^66s\ ^1S_0$ (peak 2). This disagrees with the hypothesis that the spin-flip transition is less favorable than the parallel-spin transition and leads to the much higher transition rate of the triplet state than the singlet state. The same effect is seen also for the $5s5p^66p$ states as the rates of the states which have dominant triplet character (peaks 3 and 5) are much higher than the transition rate of the state having dominant singlet character (peak 4). The SC calculations for the Rb (not shown in table) give similar results as for Cs. The calculated results disagree with the experimental find-

TABLE III. Coulomb matrix elements M, CI mixing coefficients (intermediate coupling eigenvector components) c, and Auger amplitudes of the most prominent components in Auger transitions to the $5s^25p^5(^2P_{1/2,3/2})$ final states ($c_{f\mu}=1.000$) for Cs calculated with the COWAN code. The peak labels refer to Fig. 2 and Table II.

Φ_ν	$M^{\mu\nu}_{f\beta}$	Peak 1 ($J_\beta=1$)		Peak 2 ($J_\beta=0$)	
	εp	$c_{\beta\nu}$	$c_{f\mu}c_{\beta\nu}M^{\mu\nu}_{f\beta}$	$c_{\beta\nu}$	$c_{f\mu}c_{\beta\nu}M^{\mu\nu}_{f\beta}$
$5s^{-1}6s$, $^3S_1$	−7.129	0.723	−5.154		
$5p^{-2}(^1D)5d6s$, $^3S_1$	3.277	0.669	2.193		
$5s^{-1}6s$, $^1S_0$	1.121			0.731	0.819
$5p^{-2}(^1D)5d6s$, $^1S_0$	6.867			0.664	4.558
$\|\Sigma_\mu\Sigma_\nu c_{f\mu}c_{\beta\nu}M^{\mu\nu}_{f\beta}\|^2$	SC		50.823		1.257
	CI		8.767		28.916

Φ_ν	$M^{\mu\nu}_{f\beta}$		Peak 3 ($J_\beta=0$)		Peak 3 ($J_\beta=1$)		Peak 4 ($J_\beta=1$)		Peak 5 ($J_\beta=2$)	
	εs	εd	$c_{\beta\nu}$	$c_{f\mu}c_{\beta\nu}M^{\mu\nu}_{f\beta}$	$c_{\beta\nu}$	$c_{f\mu}c_{\beta\nu}M^{\mu\nu}_{f\beta}$	$c_{\beta\nu}$	$c_{f\mu}c_{\beta\nu}M^{\mu\nu}_{f\beta}$	$c_{\beta\nu}$	$c_{f\mu}c_{\beta\nu}M^{\mu\nu}_{f\beta}$
$5s^{-1}5p^66p$, $^3P_0$	0.718	−5.638	0.725	−3.569						
$5p^{-2}(^1D)5d6p$, $^3P_0$	−0.107	2.282	0.661	1.439						
$5s^{-1}5p^66p$, $^3P_1$	0.718	−5.638			0.710	−3.491	−0.158	0.776		
$5p^{-2}(^1D)5d6p$, $^3P_1$	−0.107	2.282			0.646	1.406	−0.141	−0.308		
$5s^{-1}5p^66p$, $^1P_1$	−0.094	−0.642			0.152	−0.112	0.717	−0.528		
$5p^{-2}(^1D)5d6p$, $^1P_1$	−0.312	6.019			0.137	0.784	0.638	3.643		
$5s^{-1}5p^66p$, $^3P_2$	0.718	−5.638							0.729	−3.585
$5p^{-2}(^1D)5d6p$, $^3P_2$	−0.107	2.282							0.661	1.439
$\|\Sigma_\mu\Sigma_\nu c_{f\mu}c_{\beta\nu}M^{\mu\nu}_{f\beta}\|^2$	SC			24.206		24.544		0.204		24.206
	CI			4.537		1.996		12.837		4.607

ings. The conclusion is that the lifetime broadenings cannot be explained using the SC approximation.

Next, the broadenings generated by CI were investigated. In CI approximation, the $5s5p^66s/6p$ and $5s^25p^45d6s/6p$ configuration states having the same parity and the same total angular momenta were allowed to mix. The mixing coefficients of the most prominent components in the initial-state wave functions are given in column $c_{\beta\nu}$ in Table III. The column $c_{f\mu}c_{\beta\nu}M^{\mu\nu}_{f\beta}$ gives the Auger amplitude of each contributing component. The Auger transition rate is proportional to the squared sum of the Auger amplitudes, which is the value given in the row labeled with CI in Table III.

The Auger transition rates of the $5s5p^66s$ states will be discussed first: according to the CI calculations, the triplet state consists of the $5s5p^66s$ $^3S_1$ and $5p^4(^1D)5d6s$ $^3S_1$ components. The Auger amplitudes of the $^3S_1$ components are opposite in sign, so they partly cancel each other. This decreases the Auger transition rate of peak 1 when compared to the SC calculations. The Auger transition rate of the singlet state is, instead, increased in the CI calculations. The singlet state is contributed by the $5s5p^66s$ $^1S_0$ and $5p^4(^1D)5d6s$ $^1S_0$ components. The Auger amplitudes of the $^1S_0$ components have equal signs and the Auger amplitude of $5p^4(^1D)5d6s$ $^1S_0$ is high. As a result, the Auger transition rate of peak 2 is higher than the transition rate of peak 1, which is in agreement with the experimental findings. It was found that the electron correlation interchanges the transition

rates of the $5s^{-1}$ multiplet states increasing the broadening of the singlet state and decreasing the broadening of the triplet state.

For the laser-excited states (peaks 3–5), the mixing between the $5s5p^66p$ and $5p^4(^1D)5d6p$ states is very strong. For peaks 3 ($J=0$), 3 ($J=1$) and 5, which have a dominant triplet character, the Auger amplitudes of the "main" $5s5p^66p$ $^{2S+1}L_J$ component and the mixing $5p^4(^1D)5d6p$ $^{2S+1}L_J$ component are of the same order of magnitude but opposite in sign, which decreases the Auger transition rate. Also the Auger amplitudes of the components of peak 4 having a dominant singlet character have opposite signs. However, because the Auger matrix element between the $5p^4(^1D)5d6p$ $^1P_1$ and $5s^25p^5\varepsilon d$ ($J=1$) states is almost seven times bigger than the Auger amplitude of the $5s5p^66p$ $^1P_1$ state, the Auger transition rate of peak 4 increases remarkably when CI is taken into account in calculations. The calculated results are in agreement with the experimental results since peak 4 is wider than peaks 3 and 5.

Since the CI approximation was found to predict the Auger transition rates better than the SC approximation, the lifetime widths of the $5s^{-1}$ states of Cs and the $4s^{-1}$ states of Rb were calculated using the CI approximation in predicting the initial states. The calculated linewidths, determined with the aid of the Auger transition rates to the ns^2np^5 ($n=4$ for Rb and $n=5$ for Cs) states, are given in Table I next to the experimental values. There is a deviation between the experi-

mental and the calculated widths of peak 3 because the peaks having $J=0$ and $J=1$ cannot be separated from each other in the experimental spectrum. The calculations underestimate the transition rates from the $^1P_1$ state, especially for Rb. Generally, the calculated linewidths agree well with the experimental values, which confirms that the different lifetime widths of the photolines are explained mainly by the subsequent Auger decay rates. The CI between the $5s^{-1}$ and $5p^{-2}5d$ configurations was found to be essential in predicting the lifetime broadenings.

V. CONCLUSION

The lifetime widths of the $5s$ photolines for free Cs atoms were determined from the synchrotron radiation excited photoelectron spectrum. A part of the sample atoms were in the $[Xe]6p_{1/2,3/2}$ states due to laser excitation. The lifetime widths of the $5s5p^66l$ ($l=s$ or p) multiplets were found to be very different, with the singlet states being about three times wider than the triplet states. A similar finding was obtained previously for the $4s$ photolines of Rb [5]. The lifetime widths of the $5s$ ($4s$) photolines of Cs (Rb) are determined mainly by the Auger transition rates of the subsequent Coster-Kronig transitions to the ns^2np^5 states, where $n=5$ for Cs and 4 for Rb. The SC calculations were found to predict the lifetime widths incorrectly. By taking the electron correlation into account by allowing CI between the $5s5p^66l$ and $5s^25p^45d6l$ ($l=s$ or p) states, the prediction was improved significantly. It was found that the $5s5p^66s$ $^1S_0$ and $^3S_1$ states mix heavily with the $5s^25p^4(^1D)5d6s$ $^1S_0$ and $^3S_1$ states, respectively, via configuration interaction. The Auger transition rate of the singlet state is increased by CI and the rate of the triplet state is decreased. Electron correlation was found to affect the lifetime widths of the $5s5p^66p$ states as well. The lifetime widths of the $4s$ photolines of Rb were also predicted well by CI calculations. In conclusion, the different lifetime widths of the $5s^{-1}$ ($4s^{-1}$) multiplet photoelectron lines of Cs (Rb) originate from the electron-correlation effects.

[1] A. G. Kochur, I. D. Petrov, J. Schulz, and Ph. Wernet, J. Phys. B **41**, 215002 (2008).

[2] H. Ogasawara, A. Kotani, and B. T. Thole, Phys. Rev. B **50**, 12332 (1994).

[3] Ch. Gerth, K. Godehusen, M. Richter, P. Zimmermann, J. Schulz, Ph. Wernet, B. Sonntag, A. G. Kochur, and I. D. Petrov, Phys. Rev. A **61**, 022713 (2000).

[4] A. Sankari, R. Sankari, S. Heinäsmäki, M. Huttula, S. Aksela, and H. Aksela, Phys. Rev. A **77**, 052703 (2008).

[5] J. Schulz, E. Loos, M. Huttula, S. Heinäsmäki, S. Svensson, S. Aksela, and H. Aksela, EPL **83**, 53001 (2008).

[6] R. D. Cowan, *The Theory of Atomic Structure and Spectra* (University of California, Berkeley, CA, 1981), p. 731.

[7] A. Mäntykenttä, H. Aksela, S. Aksela, J. Tulkki, and T. Åberg, Phys. Rev. A **47**, 4865 (1993).